Available online at www.sciencedirect.com
SCIENCE DIRECT®

Journal of the European Ceramic Society 23 (2003) 2153–2161
www.elsevier.com/locate/jeurceramsoc

Formation mechanisms and morphological changes during the hydrothermal synthesis of $BaTiO_3$ particles from a chemically modified, amorphous titanium (hydrous) oxide precursor

Jooho Moon[a,*], Ender Suvaci[b], Augusto Morrone[c], Stephen A. Costantino[d], James H. Adair[e]

[a]*Department of Ceramic Engineering, Yonsei University, Seoul 120-749, South Korea*
[b]*Department of Ceramic Engineering, Anadolu University, Eskisehir 26470, Turkey*
[c]*Department of Materials Science and Engineering, University of Florida, Gainesville, FL 32611, USA*
[d]*Cabot Performance Materials, Boyertown, PA 19512, USA*
[e]*Materials Research Laboratory, The Pennsylvania State University, University Park, PA 16802, USA*

Received 5 July 2002; received in revised form 10 December 2002; accepted 1 January 2003

Abstract

The formation mechanism of $BaTiO_3$ under hydrothermal conditions was investigated. A coprecipitated precursor prepared from chemically modified titanium isopropoxide with acetylacetone and barium acetate was used as a starting material. A solid-state kinetic analysis, supported by microstructural evidence, indicates that the formation mechanism of $BaTiO_3$ in the current material system is dissolution and precipitation. The Ba–Ti complex gel dissolves into the aqueous soluble species, followed by direct precipitation from supersaturated solution. It is proposed that crystallization is controlled by dissolution of the hydrous Ti gel at the initial stage and then possibly by dissociation of the acetylacetonate group from the Ti solution species in which the acetylacetonate group is strongly bound to Ti.

Keywords: $BaTiO_3$ and titanates; Electron microscopy; Powders-chemical preparation; Hydrothermal methods

1. Introduction

Barium titanate is used as a primary material in a variety of applications including multilayer capacitors, thermistors, and electro-optic devices due to its outstanding dielectric and ferroelectric properties.[1,2] In addition to solid state synthesis,[3] barium titanate powder has been successfully synthesized by solution synthesis methods at temperatures ranging from 30 to 500 °C.[4–9] In those studies, an aqueous suspension of a mixture of hydrous Ti gel ($TiO_2{\cdot}xH_2O$) or anhydrous TiO_2, and barium salts has been used as the starting materials.[4–10] In addition, Bagwell et al. investigated the synthesis of $BaTiO_3$ from anatase and barium hydroxide octahydrate in water at 90 °C in the presence of polyacrylic and polyethylene oxide-block-polymethacrylic acids.[11] The polymers affected the morphological evolution of the forming powder by preferential adsorption on specific habit planes. The polymeric species also inhibited the formation of barium titanate. Recently, we have shown that the introduction of titanium isopropoxide modified by addition of acetylacetone to barium acetate in the hydrothermal synthesis leads to formation of $BaTiO_3$ at temperatures as low as 50 °C.[12]

Hydrothermal processing is a technique that can produce either large single crystals or fine submicron ceramic powders, depending on the apparatus configuration and the material system.[13] Hydrothermal particle synthesis involves treatment of aqueous solutions or suspensions of precursors at elevated temperature and pressure. Powders produced by this method have been demonstrated to be highly reactive toward sintering.[14] In addition, this technique possesses the potential to produce crystalline powders with controlled particle

* Corresponding author. Tel.: +82-2-2123-2855; fax: +82-2-365-5882.
E-mail address: jmoon@yonsei.ac.kr (J. Moon).

0955-2219/03/$ - see front matter © 2003 Elsevier Science Ltd. All rights reserved.
doi:10.1016/S0955-2219(03)00016-5

size, controlled stoichiometry, and, in some cases, controlled particle shape.[15] To ensure control over such particle characteristics in a given material system, particle formation mechanisms must be well understood. However, understanding the hydrothermal reaction is complex and requires a fundamental knowledge of the interactions among solid-state chemistry, interfacial reactions and kinetics, and solution chemistry. In particular, the closed reaction nature of the hydrothermal process conducted at elevated temperature and pressure makes it difficult to identify solution species and to study reaction kinetics and underlying mechanisms.[16]

The synthesis conditions for phase-pure barium titanate from aqueous solution can be inferred from phase stability diagrams.[17] This indicates the ranges of pH and barium concentrations for which $BaTiO_3$ predominates in the system at a given temperature and pressure. Recently, Lencka and Riman generated a phase stability diagram for the Ba–Ti–H_2O system based on thermodynamic calculations.[10,18] It was predicted that $BaTiO_3$ is more stable in an alkaline environment, forming in the pH range from 9 to 14 under appropriate conditions of temperature, Ba^{2+} concentration, and CO_2 content. In this regard, the thermodynamic foundation for the Ba–Ti hydrothermal system is relatively well established. However, detailed reaction pathways by which the transformation proceeds are not well recognized.

Dynamic interactions between titania, Ba^{2+}, and the surrounding solution during hydrothermal treatment lead to the crystallization of barium titanate. Two formation mechanisms have been described for hydrothermal synthesis.[19] The first is dissolution and precipitation, in which Ba^{2+} aqueous species react with hydrolyzed Ti species such as $[Ti(OH)_6]^{2-}$ or $[Ti(OH)_4^o]$ to form nuclei.[4–6] The nucleation can occur either homogeneously from bulk solution or heterogeneously at the surface of crystalline TiO_2 or related amorphous phases. Since homogeneous nucleation requires relatively high supersaturation conditions, it is more likely to occur when highly reactive and relatively soluble hydrous Ti gel is involved. On the other hand, heterogeneous nucleation, in which a solid surface locally dissolves and reacts with Ba^{2+}, will predominate when a sparingly soluble, crystalline TiO_2 precursor is used in the hydrothermal synthesis.[6,7] The second mechanism is in situ transformation, which involves diffusion of Ba^{2+} into the undissolved TiO_2 oxide, resulting in an outside layer of $BaTiO_3$ with an unreacted TiO_2 core.[20–22] Hertl[20] proposed a topochemical process in which the rate limiting step is the reaction between Ba^{2+} and TiO_2 at the interface, and the kinetic rate depends on the available surface area of TiO_2. However, as yet there has been no direct evidence to differentiate these mechanisms. One of the most extensive studies on kinetics and mechanisms of hydrothermal synthesis of barium titanate has been reported by Eckert et al.[7] In that study, barium hydroxide octahydrate and anatase titania were reacted for varying durations (1–72 h). The Johnson–Mehl–Avrami equation was used to analyze the kinetics data obtained by X-ray diffractometry and inductively coupled plasma spectroscopy. The kinetic analysis revealed two reaction-rate regimes. Although the kinetic analysis yielded insight into the first-reaction rate regime which was controlled by dissolution-precipitation mechanism, it was inconclusive in the analysis of the second-reaction rate regime.

Low temperature synthesis processes recently reported allows easier sampling throughout the reaction to monitor crystallization behavior and makes it possible to observe microstructural evidence for the reaction mechanism.[19,21,23] In the current paper, the reaction kinetics of $BaTiO_3$ nucleation and growth from such precursors under hydrothermal conditions are investigated by both analyzing the reaction kinetics and monitoring microstructure evolution.

2. Experimental procedure

Hydrous coprecipitated gel suspension was prepared as described in an earlier report.[12] 1.0 M KOH solution was used to precipitate the hydrous gel from the Ba–Ti precursor sol solution. The precursor suspension was above pH 14 and the feedstock concentration was 0.1 M. To monitor the progress of crystallization below 100 °C, a 600 ml teflon reaction vessel fitted with a condenser, thermocouple, gas inlet, and sampling dip tube was used. The teflon reactor was submerged in an oil bath which was heated using a hot plate. The reaction was performed at 75 °C by adding precursor suspension into the hot reaction vessel under an Ar environment to minimize CO_2 contamination. A stabilized reaction temperature was reached after 25 min, and this point was taken as zero time so that only isothermal reactions would be included in the kinetic analysis. Samples (4 ml) were collected by syringe throughout the duration of the process, with the temperature and pH of the supernatant recorded for each extracted sample. In the case of the kinetic study for reaction at 150 °C, a 600 ml stainless steel autoclave with a sampling capability was used. The solid portion was immediately separated from the mother liquor by centrifugation followed by repeated washing with CO_2-free deionized water (adjusted to pH 9.5–9.6) to remove the unreacted Ba species. The degree of crystallinity of the product solids were determined by weight-averaged integrated intensity of the (110, 101) X-ray reflection using the rigorous internal-standard method of Alexander and Klug.[24] Commercial barium titanate (BT–10, Cabot Performance Materials, Boyertown, PA) and starting precursor gels were used as the reference materials for the fully reacted product and unreacted materials,

respectively. Reaction products collected at various reaction times were examined by analytical transmission electron microscopy (TEM) (Jeol 200CX, Jeol USA, Boston, MA) and high resolution TEM (HRTEM) (Jeol 4000FX, Jeol USA, Boston, MA).

3. Results and discussion

3.1. Synthesis of $BaTiO_3$

Detailed conditions of the extracted samples including reaction time, temperature, and pH of the mother liquor are summarized in Table 1. X-ray powder diffraction (XRD) patterns for the $BaTiO_3$ crystallization process at 75 °C as a function of reaction time are presented in Fig. 1. The starting precursor was amorphous, transforming into crystalline $BaTiO_3$ as the reaction proceeded. After 12 min at 75 °C, barium titanate peaks begin to appear in the X-ray diffraction pattern (Fig. 1). Intensity of the $BaTiO_3$ peak increases with reaction time, suggesting that the crystallization continues even after 60 min at 75 °C.

The degree of crystallization in a material can be represented by the gross intensity (I_{gross}) associated with the area under the XRD peak. The gross intensity is defined as:

$$I_{gross} = (\text{integrated phase counts/scan time}) \times (\Delta 2\theta) \quad (1)$$

The gross intensity of the (110, 101) reflection in the 2θ range from 30.2 to 32.5° for each extracted sample was determined. The crystallization behavior of barium titanate at the two different reaction temperatures of 75 and 150 °C is shown in Fig. 2. The kinetic curve at 75 °C exhibits an induction period of approximately 10 min, followed by rapid crystallization and then decreasing conversion rate. The reaction was complete within 2 h at 75 °C. Much faster crystallization behavior was observed at 150 °C without an observable induction period. This is probably because formation of $BaTiO_3$ occurs during heat-up to the 150 °C reaction temperature. Thus, phase-pure $BaTiO_3$ with the cubic perovskite structure can be synthesized within 5 min at 150 °C.

Table 1
Kinetic data for the barium titanate formation process at 75 °C

Sample	Reaction time (min)	Temperature (°C)	Supernatant pH	Fractional crystallinity
BK-01	0	75	13.95	0
BK-02	1	75	13.94	0
BK-03	2	75	13.94	0
BK-04	3	76	13.93	0
BK-05	4	76	13.93	0
BK-06	5	76	13.92	0
BK-07	8	75	13.92	0
BK-08	10	75	13.91	0
BK-09	12	75	13.91	0.220
BK-10	15	75	13.90	0.350
BK-11	17	75	13.90	0.409
BK-12	19	75	13.89	0.490
BK-13	22	75	13.89	0.650
BK-14	25	75	13.88	0.795
BK-15	35	75	13.87	0.825
BK-16	45	75	13.86	0.862
BK-17	60	75	13.83	0.916
BK-18	100	75	13.80	0.970

3.2. Kinetic analysis of $BaTiO_3$ formation

In order to gain further insight into the formation mechanism of crystalline $BaTiO_3$, a kinetic analysis was performed on the crystallization kinetic data using the Johnson–Mehl–Avrami equation:[25]

$$\ln[-\ln(1-f)] = \ln(r) + m\ln(t) \quad (2)$$

where f is the fraction crystallized isothermally at time t, r is the rate constant which partially depends on nucleation frequency and growth rate and is very sensitive to temperature, and m is the exponent constant which is independent of temperature but sensitive to the time dependence of the nucleation and growth rate and to the geometry of the particle. Hancock and Sharp have shown that for reactions obeying a single theoretical rate expression, plots of $\ln[-\ln(1-f)]$ against $\ln(t)$ over the range $f = 0.15$–0.50 yield approximately straight lines, with slopes characteristic of three distinct reaction mechanisms.[16,26,27] When $m = 0.54$–0.62, diffusion is the rate limiting step, while for $m = 1.0$–1.24, a zero-order, first-order, or phase boundary controlled mechanism is indicated. A mechanism involving nucleation and growth control is implied when $m = 2.0$–3.0.

In the current research, kinetic analysis was applied only to the kinetic data obtained at 75 °C due to the lack of early crystallization data for the 150 °C reaction (initial fractional crystallinity > 0.7). The results of the kinetic analysis are presented in Fig. 3. The crystallization kinetics are described by a two-stage kinetic rate law similar to that observed by Rosetti et al. for lead titanate,[16] and more recently by Eckert et al. for barium titanate from crystalline TiO_2 precursor.[7] The first stage is characterized by $m = 2.30$, followed by a transition at approximately $f = 0.6$ to a second stage in which $m = 0.70$. The formation kinetics of the first stage are characteristic of a nucleation and growth mechanism, indicating that the product phase is growing from randomly distributed nuclei within the reactant phase. The m value for the second region is not characteristic of any of the three mechanisms. The solid state nature of the transformation implies that the dissolution and precipitation mechanism operates in the solution phase.

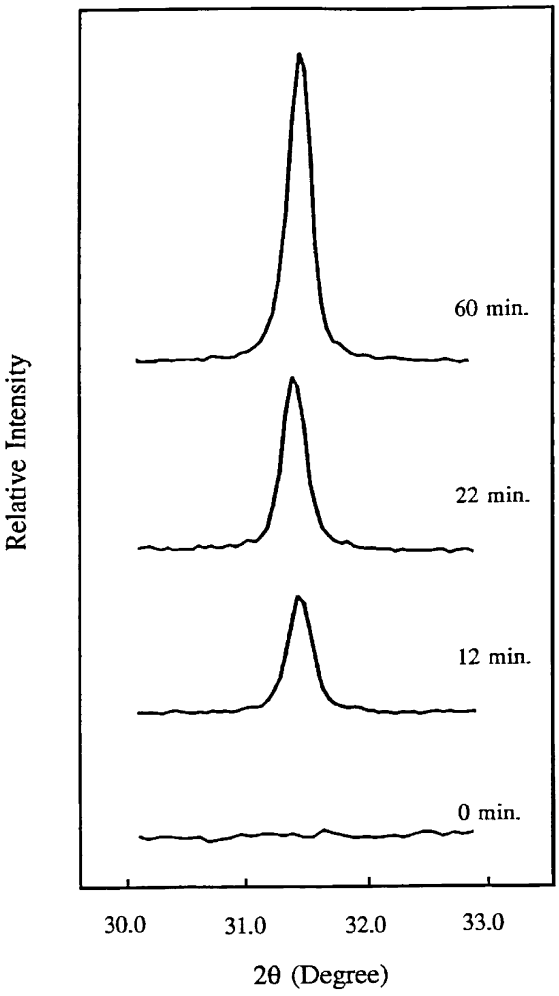

Fig. 1. X-ray diffraction patterns of (110, 101) reflection showing a change in crystallinity as a function of reaction time during the barium titanate formation process at 75 °C.

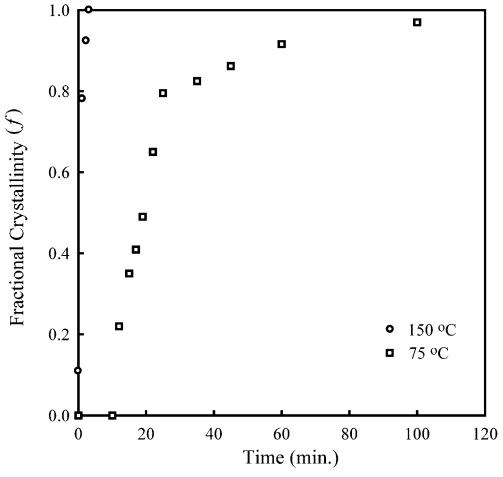

Fig. 2. Crystallization curves for $BaTiO_3$ produced under hydrothermal conditions.

However, the Hancock and Sharp kinetic analysis was originally designed for isothermal solid-state transformation such as the dehydroxylation of brucite,[26] and it is difficult to achieve literal mechanistic interpretation based only on the m values. Morphological analyses discussed in the next section are required to fully deduce the reaction kinetics as shown previously by Eckert et al.,[7] Kerchner et al.,[19] and MacLaren et al.[21]

3.3. Morphological analysis of $BaTiO_3$ formation

To minimize the limitations associated with the Hancock and Sharp kinetic analysis, the above results were correlated with microstructural evidence from the TEM studies for the crystallization process at 75 °C. Fig. 4 presents electron micrographs showing the barium titanate formation process as a function of reaction time. Crystalline $BaTiO_3$ particles of approximately 50 nm diameter were observed after 5 min, although crystallinity in this sample could not be detected by XRD analysis. These particles grew to 80 nm during the course of the 60 min reaction. Interestingly, some particles at the intermediate stage exhibited a faceted cubic shape. The cubic morphology reflects the crystallographic nature of the pseudocubic perovskite produced by hydrothermal synthesis.

HRTEM was used to investigate the nucleation process and morphological features of nuclei in the samples collected before the reaction temperature stabilized. For the sample extracted at the instantaneous temperature of 42 °C, 5 min after the precursor solution was added into the reactor, spherical nuclei approximately 4 nm in size were observed, as shown in Fig. 5(a). It was difficult to obtain the focused image of a single nuclei with an electron beam strength of 400 kV due to interactions

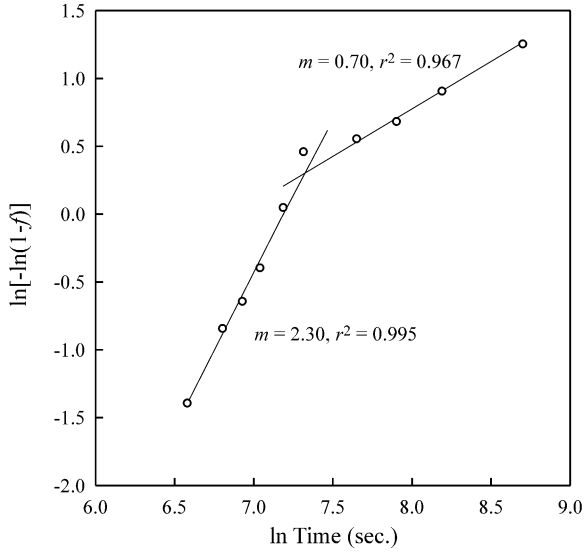

Fig. 3. Johnson–Mehl–Avrami plot for the kinetic data of $BaTiO_3$ formation at 75 °C, where m is the exponent constant and r^2 is the correlation coefficient.

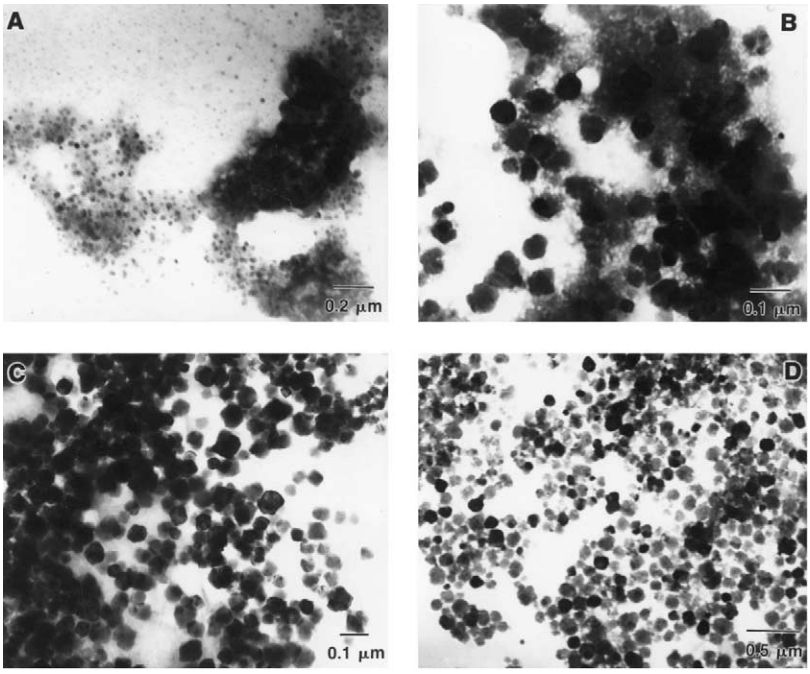

Fig. 4. TEM micrographs showing the formation process of $BaTiO_3$ at 75 °C as a function of reaction time: (a) 5 min (BK-06); (b) 15 min (BK-10); (c) 25 min (BK-14); and (d) 60 min (BK-17), respectively.

between the nuclei and electron beam. Even with an electron beam voltage of 200 kV, the diffraction pattern from a particular area had changed after 4 min of electron beam exposure. The origin of this interaction is presumably related to destruction or displacement of the nuclei by the strong focused electron beam. Despite this problem, several nuclei clearly show a lattice structure. Selected area diffraction analysis of $BaTiO_3$ nuclei reveals their single-crystal nature, as shown in Fig. 5(b). The crystal structure of the nuclei is consistent with the pseudo-cubic phase usually associated with hydrothermal barium titanate.[28]

3.4. Proposed mechanism for $BaTiO_3$ formation

Two models have been proposed in the literature to describe the room temperature stabilization of the cubic phase based on either a cubic surface layer or a strain effect model in which lattice hydroxyl groups and particle size play an important role.[28,29] Since the formation of an interface of crystal structural transition within such a small nuclei is unlikely, the latter mechanism is considered to be appropriate here. Furthermore, it was observed that lattice fringes pass across the entire crystallite without interruption, indicating that the nuclei are free from any point or line defects and are neither partially nor poorly crystallized, as would be expected in the product from homogeneous precipitation. The HRTEM micrograph in Fig. 6 shows the microstructural features of sample BK-06, which was grown for a further 5 min at 75 °C. Microstructural information revealed by the lattice structure implies that the particles have a very clear boundary without any amorphous surface layer and still maintain a defect-free structure. Unlike the initial nuclei observed in sample BK-01, the particle morphology for BK-06 is cubic. However, for the fully grown barium titanate particles the dominant morphology is spherical.[12] Thus it appears that morphological changes occur during the growth process. The originally spherical particles transform to a cubic morphology and later revert to the spherical habit.

Spherical $BaTiO_3$ nuclei form in order to minimize the surface area in the nucleation process. As such nuclei grow, crystallographic habit growth causes the spherical nuclei to develop into cubic particles. In the perovskite structure, the {100} plane has the lowest surface energy and in turn the slowest planar growth rate.[30] Thus, the equilibrium shape is cubic, as observed in other perovskites such as $PbTiO_3$ and PZT.[31–33] However, the high energy faceted edges of the cubic particles may be subject to preferential dissolution and, in addition, the strain associated with cubic structure stabilization tends to reduce the surface area of the growing particles. As a result, the intermediate morphology consists of cubic particles with the spherical shape regained during the final stage of growth, although some larger particles still retain their cubic shape. The particle surface roughness shown previously,[12] is probably a result of this competing effect between growth rate and edge effects.

This microstructural evidence, combined with the Johnson–Mehl–Avrami kinetic analysis, strongly supports

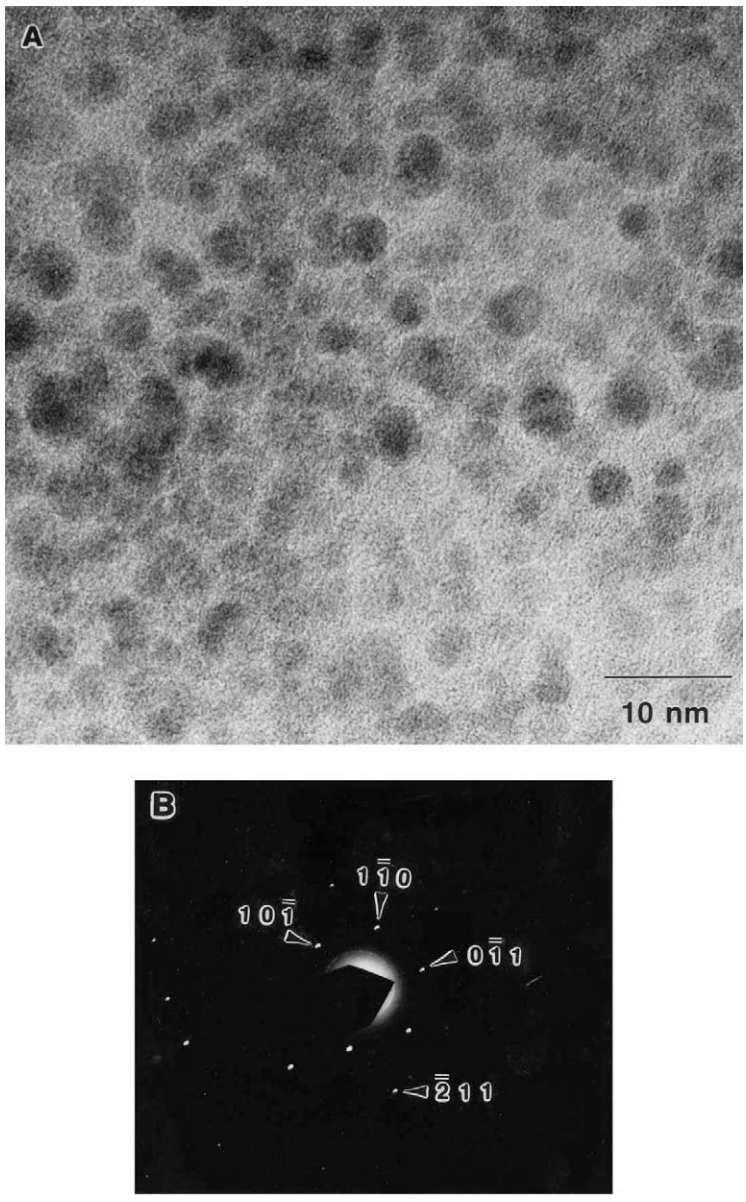

Fig. 5. HRTEM micrographs of the sample BK-01 including a selected area diffraction pattern (zone axis [111]).

the contention that the formation mechanism of $BaTiO_3$ in the current material system is dissolution and precipitation as previously observed by Pinceloup et al.[23] If transformation is achieved by inward diffusion into the undissolved amorphous Ti gel structure, the boundary between the unreacted Ti gel core and the $BaTiO_3$ outside layer should be observed at the early stage of nucleation by HRTEM. However, MacLaren and Ponton have proposed based on HRTEM study together with EDX analysis that the formation mechanism of barium titanate from a hydrous Ti gel in a solution of barium acetate and the organic base is in situ transformation.[21] They have observed that Ba ions diffuse into the gel, resulting in the formation of nanosized crystallites at 40 °C, which grow into larger particles by aggregation during further heat treatment. This discrepancy is probably associated with the incorporation of acetylacetonate-modified titanium isopropoxide within the current hydrothermal particle synthesis. Strong complexing ability of acetylacetone should promote solubility of hydrous acetylacetonate– TiO_2 gel as thermodynamically predicted in an earlier report.[33] Highly reactive acetylacetonate–TiO_2 gel can dissolve readily even at lower temperatures ~40 °C in a highly alkaline condition, forming a supersaturated condition sufficient for precipitation from homogenous solution. This leads to a different formation mechanism of barium titanate even though similar hydrothermal reaction conditions are involved in both studies.

To describe the relevant reaction for the proposed formation mechanism, $BaOH^+$ and $Ti(OH)_4^0$ are taken to be the appropriate solution reacting species involved

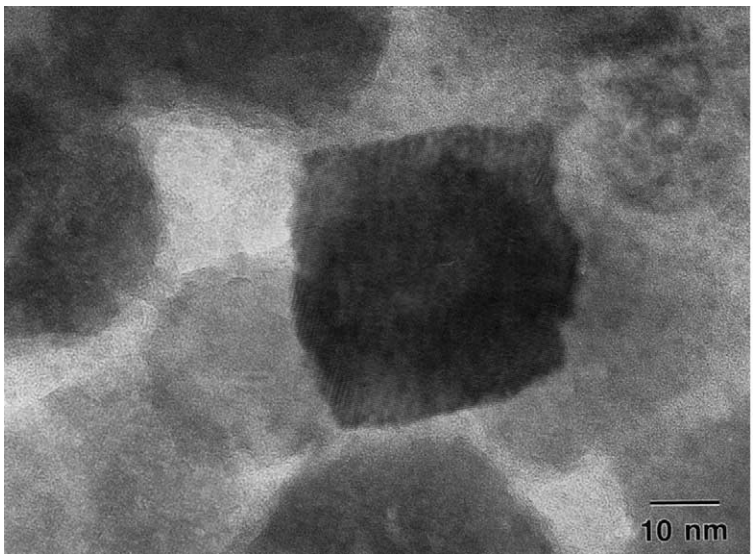

Fig. 6. HRTEM micrograph of sample BK-06.

in the current highly alkaline condition, as indicated by thermodynamic calculations in the $BaTiO_3$ phase stability diagram.[10,17,18] $BaTiO_3$ precipitates from solution via the following reactions:

$$BaTi(OH)_xO_y(acac)_{z(s)} \leftrightarrow BaOH^+_{(aq)} + Ti(OH)^0_{4(aq)} + H_2O_{(1)} + acacH \quad (3)$$

$$BaOH^+_{(aq)} + Ti(OH)^0_{4\,(aq)} \leftrightarrow BaTiO_{3\,(s)} + 2H_2O_{(1)} + H^+_{(aq)} \quad (4)$$

It was shown in our previous paper that pH is a critical reaction parameter in synthesizing phase-pure $BaTiO_3$ under hydrothermal conditions in the acetylacetonate-modified system.[12] The presence of OH^- ions is required to form the hydrolyzed aqueous species and subsequently to enhance precipitation of the crystalline product from the Ba–Ti amorphous complex gels. According to the reactions shown in Eqs. (3) and (4), H^+ ions are released as barium titanate forms, resulting in a decrease in pH. Accordingly, the pH of the reaction medium decreases steadily during the reaction, becoming constant upon reaction completion.

Precipitation from solution proceeds through (i) formation of solute species, (ii) nucleation from the supersaturated solution, and (iii) particle growth via either solute addition reaction or aggregation.[34] In the current system, the formation of solute species occurs via dissolution of the hydrous Ba–Ti gel as indicated by Eq. (3). Once the solution is supersaturated due to dissolution of the precursor, precipitation of $BaTiO_3$ from homogeneous solution occurs, resulting in an abundance of nuclei. The dissolution of the hydrous titania is the rate limiting step in the early stage of nucleation and growth. After nucleation, the nuclei grow rapidly, resulting in a fast initial rate in the crystallization kinetics curve as observed in Figs. 2 and 3. The solute concentration decreases to below critical supersaturation as a result of the nucleation event, but remains sufficiently high for the particles to grow without secondary nucleation. If the particles grew by aggregation, defect structures such as stacking faults or grain boundaries should exist.[9] However, HRTEM analysis does not reveal any evidence of the presence of aggregated particles. Lack of defects supports the notion the particles grow by the addition of solute. This reaction is controlled either by diffusion or by a surface incorporation reaction. In the current system, growth rate is more likely to be controlled by slower surface reactions due to the high diffusion coefficient of the solute in solution phase under hydrothermal conditions. Although $[Ti(OH)^0_4]$ is assumed to be the soluble species for Ti, different soluble species of Ti such as $Ti(OH)_{4-x}(acac)_x$, in which the acetylacetonate group is strongly bound to Ti, also exist.[4,12] If such solute species are involved in a surface reaction with Ba^{2+}, the acetylacetonate group must be released during the dehydration process prior to the incorporation step at the surface of the growing particle. Therefore, the dissociation of this terminal group can be rate-limiting in the later stage of growth, which provides a slower kinetic rate in the final stage as shown in Fig. 2.

4. Conclusions

Formation mechanisms of $BaTiO_3$ under hydrothermal conditions were investigated. The use of the coprecipitated precursor prepared from modified titanium alkoxide and barium acetate enabled the crystallization

behavior at 75 °C to be monitored. Spherical, 4 nm diameter nuclei formed at lower temperatures in the reacting system were observed using high resolution TEM. The lattice image of the 4 nm nuclei implies that the crystallites have a defect-free structure and are not either partially or poorly crystallized. The morphology of the nuclei changes to cubic in an intermediate particle formation stage, then generally returns to spherical when the reaction is complete. A solid-state kinetic analysis, supported by microstructural evidence, indicates that the formation mechanism of $BaTiO_3$ in the current material system is dissolution and precipitation. The Ba–Ti complex gel dissolves into the aqueous soluble species, followed by direct precipitation from supersaturated solution. It is proposed that crystallization is controlled by dissolution of the hydrous Ti gel at the initial stage and then possibly by dissociation of the acetylacetonate group from the Ti solution species in which the acetylacetonate group is strongly bound to Ti.

Acknowledgements

The authors gratefully acknowledge the support of this work by Cabot Performance Materials Inc., Boyertown, PA. The authors would also like to thank the Major Analytical Instrumentation Center (MAIC) at the University of Florida for assistance in the characterization of materials.

References

1. Cross, L. E., Dielectric, piezoelectric, and ferroelectric components. *Am. Ceram. Soc. Bull.*, 1984, **63**, 586–590.
2. Hennings, D., Barium titanate based ceramic materials for dielectric use. *Int. J. High Technol. Ceram.*, 1987, **3**, 91–111.
3. Amin, A., Spears, M. A. and Kulwicki, B. M., Reaction of anatase and rutile with barium carbonate. *J. Am. Ceram. Soc.*, 1983, **66**(10), 733–738.
4. Phule, P. P. and Risbud, S. H., Review: low-temperature synthesis and processing of electronic materials in the $BaO–TiO_2$ system. *J. Mater. Sci.*, 1990, **25**, 1169–1183.
5. Chaput, F., Boilot, J.-P. and Beauger, A., Alkoxide-hydroxide route to synthesize $BaTiO_3$-based powders. *J. Am. Ceram. Soc.*, 1990, **73**(4), 942–948.
6. Chien, A. T., Speck, J. S., Lange, F. F., Daykin, A. C. and Levi, C. G., Low temperature/low pressure hydrothermal synthesis of barium titanate: powder and heteroepitaxial thin films. *J. Mater. Res.*, 1995, **10**(7), 1784–1789.
7. Eckert, J. O. Jr., Hung-Houston, C. C., Gersten, B. I., Lencka, M. M. and Riman, R. E., Kinetics and mechanims of hydrothermal synthesis of barium titanate. *J. Am. Ceram. Soc.*, 1996, **79**(11), 2929–2939.
8. Zhao, L., Chien, A. T., Lange, F. F. and Speck, J. S., Microstructural developmnent of $BaTiO_3$ powder synthesized by aqueous methods. *J. Mater. Res.*, 1996, **11**(6), 1325–1328.
9. Her, Y-S. and Matijevic, E., Preparation of well-defined colloidal barium titanate crystal by the controlled double-jet precipitation. *J. Mater. Res.*, 1995, **10**(12), 3106–3114.
10. Lencka, M. M. and Riman, R. E., Thermodynamic modeling of hydrothermal synthesis of ceramic powders. *Chem. Mater.*, 1993, **5**, 61–67.
11. Bagwell, R. B., Sindel, J. and Sigmund, W., Morphological evolution of barium titanate synthesized in water in the presence of polymeric species. *J. Mater. Res.*, 1999, **14**(5), 1844–1851.
12. Moon, J., Suvaci, E., Li, T., Constantino, S. and Adair, J. H., Phase development of barium titanate from chemically modified-amorphous titanium (hydrous) oxide precursor. *J. Eur. Ceram. Soc.*, 2002, **22**(6), 809–815.
13. Laudise, R. A., Hydrothermal synthesis of crystals. *Chem. Eng. News*, 1987, **28**, 30–43.
14. Dawson, W. J., Hydrothermal synthesis of advanced ceramic powders. *Am. Ceram. Soc. Bull.*, 1988, **67**, 1673–1678.
15. Cho, S.-B., Sridhar, V. and Adair, J. H., Morphological forms of α-alumina particles synthesized in 1,4-butanediol solution. *J. Am. Ceram. Soc.*, 1996, **79**(1), 88–96.
16. Rossetti, G. A. Jr., Watson, D. J., Newnham, R. E. and Adair, J. H., Kinetics of the hydrothermal crystallization of the perovskite lead titanate. *J. Cryst. Growth*, 1992, **116**, 251–259.
17. Osseo-Asare, K., Arriagada, F. J. and Adair, J. H., Solubility relationships in the coprecipitation synthesis of barium titanate: heterogeneous equilibria in the $Ba-Ti–C_2O_4–H_2O$ system. In *Ceramic Transactions, Ceramic Powder Science I*. The American Ceramic Society, Inc., Westerville, OH, 1988, pp. 47–53.
18. Lencka, M. M. and Riman, R. E., Hydrothermal synthesis of perovskite materials: thermodynamic modeling and experimental verification. *Ferroelectrics*, 1994, **151**, 159–164.
19. Kerchner, J. A., Moon, J., Chodelka, R. E., Morrone, A. and Adair, J. H., Nucleation and formation mechanisms of hydrothermally derived barium titanate. In *Synthesis and Characterization of Advanced Materials. ACS Symposium Series, Vol. 681*, ed. M. A. Serio, D. M. Gruen and R. Malhotra. American Chemical Society, 1998, pp. 106–119.
20. Hertl, W., Kinetics of barium titanate synthesis. *J. Am. Ceram. Soc.*, 1988, **71**(10), 879–883.
21. MacLaren, I. and Ponton, C. B., A TEM and HREM study of particle formation during barium titanate synthesis in aqueous solution. *J. Eur. Ceram. Soc.*, 2000, **20**, 1267–1275.
22. Hu, M. Z.-C., Kurian, V., Payzant, E. A., Rawn, C. J. and Hunt, R. D., Wet-chemical synthesis of monodispersed barium titanate particles-hydrothermal conversion of TiO_2 microspheres to nanocrystalline $BaTiO_3$. *Powder Tech.*, 2000, **110**, 2–14.
23. Pinceloup, P., Courtois, C., Vicens, J., Leriche, A. and Thierry, B., Evidence of a dissolution-precipitation mechanism in hydrothermal synthesis of barium titanate powders. *J. Eur. Ceram. Soc.*, 1999, **19**, 973–977.
24. Alexander, L. and Klug, H. P., Basic aspects of X-ray absorption in quantitative diffraction analysis of powder mixtures. *Anal. Chem.*, 1948, **20**(10), 886–889.
25. Avrami, M. J., Kinetics of phase change. I. *J. Chem. Phys.*, 1939, **7**, 1103–1112.
26. Hancock, J. D. and Sharp, J. H., Method of comparing solid-state kinetic data and its applications to the decomposition of kaolinite, brucite, and $BaCO_3$. *J. Am. Ceram. Soc.*, 1992, **55**(2), 74–77.
27. Hulbert, S. F., Models for solid-state reactions in powdered compacts: a review. *J. Brit. Ceram. Soc.*, 1969, **6**, 11–20.
28. Saegusa, K., Rhine, W. E. and Bowen, H. K., Effect of composition and size of crystallite on crystal phase in barium titanate powder. *J. Am. Ceram. Soc.*, 1993, **76**(6), 1505–1512.
29. Begg, B. D., Vance, E. R. and Nowotny, J., Effect of particle size on the room-temperature crystal structure of barium titanate. *J. Am. Ceram. Soc.*, 1994, **77**(12), 3186–3192.
30. Tani, T., Xu, Z. and Payne, D., Preferred orientations for sol-gel derived PLZT thin layers. In *Ferroelectric Thin Films III, Symposium Proceedings Vol. 310*, ed. E. R. Myers, B. A. Tuttle,

S. B. Desu and .P.K. Lauser. Material Research Society, Pittsburgh, 1993, pp. 269–274.
31. Moon, J., Li, T., Randall, C. A. and Adair, J. H., Low temperature synthesis of lead titanate by a hydrothermal method. *J. Mater. Res.*, 1997, **12**(1), 189–197.
32. Beal, K. C., Precipitation of lead zirconate titanate solid solution under hydrothermal conditions. In *Advances in Ceramics, Vol 21, Ceramic Powder Science*, ed. G. L. Messing, K. S. Mazdiyasni, J. W. McCauley and R. A. Haber. The American Ceramic Society Inc, Westerville, OH, 1987, pp. 33–41.
33. Moon, J., Kerchner, J. A., Krarup, H. and Adair, J. H., Hydrothermal synthesis of ferroelectric perovskites from chemically modified titanium isopropoxide and acetate salts. *J. Mater. Res.*, 1999, **14**(2), 425–435.
34. Sugimoto, T., Preparation of monodispersed colloidal particles. *Adv. Colloid Interface Sci.*, 1987, **28**, 65–108.